COBEM 2023 27TH INTERNATIONAL CONGRESS OF MECHANICAL ENGENEERING

ABCM Brazilian Society of Mechanical Sciences and Engineering
27th ABCM International Congress of Mechanical Engineering
December 04-08, 2023, Florianópolis-SC, Brazil

COBEM2023-1718
PERFORMANCE ANALYSIS FOR A CROSS-FLOW FAN IN A HOUSEHOLD EVAPORATIVE COOLER

Matheus H. C. Garros[1]
[1]Energy Engineer and MsC student at UNICAMP – Universidade Estadual de Campinas, Campinas-SP, Brazil
matheus.garros@gmail.com

Patrick O. Guedes[2]
Robson Leal da Silva[2,3]
[2]UFGD – Grande Dourados Federal University, FAEN – College of Enginnering, Dourados-MS, Brazil
[3]PEM – Graduate Program in Mechanical Engineering, UEM – Maringá State University, Maringá-PR, Brazil
patrickog99@gmail.com
rlsilva@hotmail.com

Abstract. *Small evaporative coolers have increasing use in household appliances for thermal comfort due to their low energy consumption comparing to vapor compression refrigeration systems. Nevertheless, very little data is available to the consumers from manufacturers regarding the fan performance itself. Thus, the objective is to investigate if the amount of kinetic energy provided for a low-pressure crossflow fan (CFF) represents a significant contribution in comparison to the thermal energy available from the psychometric process by the evaporative cooler; and, to identify if maximum fan performance occurs in the angular speeds operating range and if nominal airflow values provided by the manufacturer are consistent to experimental results. The methodology considers experimental measurements for ambient conditions (pressure, temperature, and humidity), fan angular speeds, and airflow velocities at the rotor's inlet and outlet by Euler's equation. The main findings are: 1) It's not possible to identify maximum performance in the operational angular speeds; 2) The CFF kinetic energy is negligible in comparison to thermal energy in small evaporative coolers (EC); 3) Experimental results for airflow values at the rotor's maximum angular speed is consistent to nominal values provides by the manufacturer.*

Keywords: *fluid mechanics, cross-flow fan, ventilation, evaporative cooler, performance.*

1. INTRODUCTION

Fluid machines have a wide range of engineering applications in household, commercial, and industrial areas. They can be classified according to the flow direction in the rotor (or impeller): axial – when the flow is parallel to the rotation axis; centrifugal (or radial) when the flow is perpendicular; mixed when the flow has a direction between radial and axial to the rotational axis; and tangential when the flow velocity is tangent to the rotor – as hydraulic turbines Pelton and Michell-Banki, and crossflow (or tangential) fans.

Resembling axial fluid machinery, crossflow fans (also called tubular fans or blowers, shortened as CFF) provide low static pressure rise ($\downarrow \Delta p_{static}$) when the flow crosses the rotor once it has an open design that also results in low airflow rate and, as aftereffect, low efficiency. However, it provides amusing features due to its long-narrow design as space-saving, 2-D laminar airflow field across the whole length of the rotor exit, simple structure, small size, stable airflow, high dynamic pressure coefficient ($\uparrow \Delta p_{dynamic}$), and low noise.

The rotor is a drum-type with multiple forward-curved blades that move air from the inlet to the outlet side without compressing or paddling the air. Hence, low noise level and quiet operation within linear regions of airflow. It is suitable for electronics cooling and domestic applications as evaporative cooling equipment. It is also part of other equipment such as air-conditioning and heating apparatus (in-door split-type), air curtains (Dragomirescub and Ciocãnea, 2015), air purifiers, freezers, and many others.

Either CFD simulations or experimental investigations allow to determine the performance characteristics. As for similarity laws using Buckingham's theorem for non-dimensional parameters, previous research identified that the rotor dimensions and fluid viscosity (at blade reference Reynolds numbers lower than 10,000-15,000 range) affect the crossflow fan s performance curves (Tanaka and Murata, 1995). The casing geometrical characteristics (fan dimensions) also interfere with performance curves due to the resulting vortex shape (Porter and Markland, 1970). The vortex wall configuration plays a significant role, as investigated in crossflow fan applications for grain cleaning in agricultural machines, and its positioning also affects the mass flow rate division in two outlets (Gebrehiwot, Baerdemaeker, and Baelmans, 2010).

CFF energy losses and overall performance depend on the eccentric vortex or re-circulating region (completely closed streamlines). It occurs in the outlet flow due to vortex shedding at the fan blades' trailing edges (Yamafuji, 1975). The rotor influences the vortex characteristics, as long as casing and volute tongue geometry (Sun et al, 2015). As the tongue's size increases, there is noise reduction, on the other hand, a decrease in efficiency (Koo, 1999). The inlet guide vanes (IVG) design can improve CFF efficiency by reducing the flow separation (re-circulating region) and optimizing the inside flow field (through-flow). Also, the eccentric vortex region has little mass transfer with the through-flow region, i.e., inflow and outflow regions (Sun et al, 2015).

1.1 Objectives

Small evaporative coolers have increasing use in household appliances for thermal comfort due to their low energy consumption compared to vapor compression refrigeration systems, many equipped with CFF. Nevertheless, very little data are available to the consumers from manufacturers regarding the fan performance itself, usually only nominal flow rate and not even indicating if that corresponds to equipment operation with or without the water pump working. Thus, main objectives are: 1) To investigate if the amount of kinetic energy provided for a CFF is relevant compared to thermal energy from the psychometric process; 2) To identify if maximum fan performance occurs in the angular speeds operating range; 3) If nominal airflow values provided by the manufacturer are consistent with experimental results.

2. METHODOLOGY

The CFF investigated is a component in an evaporative cooler (EC) for residential use (Manufacturer: Ventisol, CLM-01). The EC indicates nominal flow rate and electrical power as 350 m³/h and 75 W (127 V e 60 Hz). The rotor is drum-type and has 35 blades equally divided into four blocks. It operates at three angular speeds (850, 960, and 1020 RPM). The EC's CFF main dimensions are shown in Table 1.

Table 1. EC's CFF dimensions

Dimension	Value (mm)
Height (h)	0.248
External diameter (D_e)	0.115
Internal diameter (D_i)	0.094
Blades width (l)	0.011
Inlet width (L_i)	0.155
Outlet width (L_o)	0.082

In correlation to the experimental results obtained, the velocity triangles proposed for the CFF model were analyzed based on the areas and blade angles shown in Figure 1.

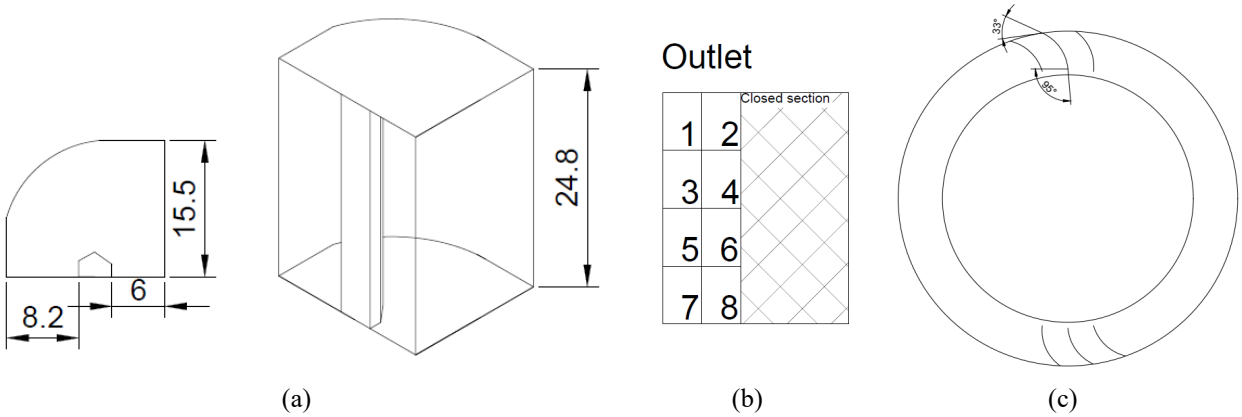

(a) (b) (c)

Figure 1. EC carcass dimensions (a), outlet area measuring positions (b) and blade angles – intel and outlet (c)

2.1 Measuring instruments and laboratory ambient conditions

During the tests the following were measured: (1) Temperature, relative humidity, and pressure at the inlet and outlet via Arduino sensor; (2) Flow speed before and after air passage through the rotor via vane anemometer; (3) Voltage and electric current via multi-meter; (4) Rotor angular speed, via tachometer. The specifications conform to Table 2.

Table 2. Instrumentation data and information

Measurement	Model	Range	Resolution	Accuracy
(1)	BME 280 (Bosch)	-40 to -85 °C; 3000 to 11000 Pa; 0 to 100%	0.01°C; 0.18 Pa; 0.008%	±1 C°; ±100 Pa; ±3%
(2)	416 (Testo)	0.6 to 40 m/s	0.1 m/s	±2m/s + 1.5%
(3)	VA-750 (Instrutherm)	1 to 1000 V; 1 to 1000 A	1 V; 100 mA	±1% (V); ±2% (mA)
(4)	TD – 813 (Instrutherm)	0.5 to 999.9 RPM	0.1 RPM	±0.05% + 1 digit

Since it was not possible to have control over ambient conditions at the test site, and with the tests lasting three days, the ambient conditions (Table 3) could have some impact on the results obtained, but as they didn't vary much, it wasn't considered on this first analysis.

Table 3. Laboratory mean ambient conditions registered during tests.

UR (%) (1)	Temperature (K)	Pressure-Barometric (Pa)
54.52 ± 3.00	293.9 ± 1.0	96885 ± 100
53.40 ± 3.00	292.2 ± 1.0	96665 ± 100
61.26 ± 3.00	297.7 ± 1.0	96126 ± 100

(1) Air Relative Humidity

2.2 Experimental procedure

During the test, for each position of Figure 1b (see positions 1 up to 8), the air velocity was measured 5 (five) times. This procedure happened for all 3 (three) rotor angular speeds. Since each selected point had a different – but almost constant value (due to the velocity profile of the EC's outlet), the chosen uncertainty – for the mean velocity, was the higher among those velocities calculated for all the positions in each rotor angular speed. The data acquisition for each measurement lasted 60 seconds, using the mean function of the anemometer. Plus, we measured the air relative humidity (inlet and outlet) and total equipment mass, to calculate the water consumption.

The decision to acquire only five measurements for each position in the outlet came after experimentation using 10 measures of the outlet flow velocity for 850 RPM, for every point. The results showed that the mean and the standard deviation were the same for 5 or 10 measurements.

2.3 Mathematical formulation (or Theoretical model – Velocity triangle) and Velocity acquisition

The mathematical formulation of the velocity triangles is based on the generic triangle shown in Figure 2. The analysis was carried out using valid trigonometric relations. ***C*** represents the absolute velocity, ***W*** is the relative velocity, and ***U*** is the rotor's tangential velocity on the analysis point. As will be discussed further, $\boldsymbol{C_m}$ is responsible for the flow rate, and $\boldsymbol{C_u}$ is a measure of energy in the flow. Since ***W*** is the relative velocity, its components represent the same, but are all relative to the rotor's movement.

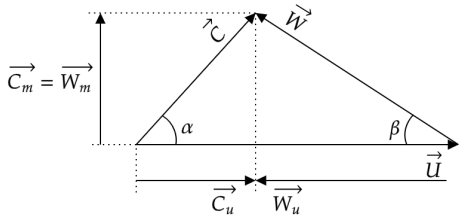

Figure 2. Generic velocity triangle

Air density can be estimated (Balbinot and Brusamarello, 2010) with Eq. (1a), where parameters must be in T_{air} (K) and p_{local} (Pa). The number 287.1 on Eq. (1b) is from the ideal gas constant.

$$\rho = \frac{p_{lab}}{RT_{air}} \tag{1a}$$

$$u(\rho) = \sqrt{\left(\frac{u(p_{lab})}{287.1T_{air}}\right)^2 + \left(\frac{p_{lab}u(T)}{287.1T_{air}^2}\right)^2} \tag{1b}$$

p_{lab}: Barometric pressure, in absolute values [Pa];
ρ_{air}: Air density [kg m^{-3}];
R: Ideal gases constant, air [287.1 J (kmol K)$^{-1}$];
T_{air}: Temperature [K];

From Eq. (1) and (2), the air density mean value and uncertainty is 1.136 ± 0.004 kg/m³, a reference value that eventually could be considered in fan characteristic curves. Standard air density is ~1.200 kg/m³ (NTP – Normal Temperature and Pressure conditions at sea level) or 5.33% difference from the result obtained in tests; thus, the results presented in this work are not corrected for volumetric flow.

The velocities measured in the outlet had its type B uncertainty estimated, associating the repeatability and instrument uncertainty (Albertazzi et al., 2018, Neto, 2012). For the 850 RPM angular speed, due to the limitation of the instrument's resolution to read the low air velocities, we decided to use the maximum speed values (within the 60 seconds test). Following Henn (2006), the component of the fluid velocity related to volumetric flow is the vertical component of C, or C_m, which is the value measured via anemometer.

The uncertainty associated with repeatability is the sample standard deviation. A probability of 95.45% (2σ) was considered, having a degree of freedom υ = 5 – 1 (4); and t = 2.869 (Student's Coefficient). Hence, the outlet velocity uncertainty can be defined by Eq. (2), noting that this is the uncertainty for just one point, and as settled before, the mean uncertainty was chosen as the maximum value for a given point, since there was a high variation of magnitude point to point, and the objective was not to take this variation into account, but the measurement uncertainty. In Eq. 2 *u(a)* represents the instrument uncertainty (anemometer).

$$u(C_m) = \sqrt{(2\sigma)^2 + \left(u(a)\right)^2} \tag{2}$$

The volumetric airflow through the fan is according to Eq. (3), relating the mean velocity to the area over which the air flows.

$$\dot{V} = \overline{C_{m,o}}A_o \tag{3}$$

$\dot{V}$: Volumetric flow [m³/s];
$\overline{C_{m,o}}$: Mean outlet meridional velocity at the outlet [m/s];
A_o: Outlet area [m²].

Power exchange and global efficiency

The specific energy exchanged between the rotor and fluid is defined by Henn (2006), considering there are no guideline blades before the rotor, so $C_{u,i}$ is approximately zero (because α angle at inlet is approximately 90º). Therefore, we can simplify the original expression to Eq. (4)

$$Y_{fluid} = U_o C_{u,o} \tag{4}$$

Y_{fluid}: Specific energy exchanged between rotor and fluid [J/kg];
$C_{u,o}$: Absolut tangential velocity at the outlet [m/s];
U_o: Rotor tangential velocity at the outlet [m/s].

The power transferred from the blades to the fluid is defined by Eq. (5):

$$P_{fluid} = \dot{m}Y_{fluid} \tag{5}$$

P_{fluid}: Power exchanged between rotor and fluid [W];

$\dot{m}$: Mass flow rate [kg/s].

The electric power demanded by the evaporative cooler (EC) is given by Eq. (6).

$$P_e = VI \tag{6}$$

P_e: Electric power of the EC [W];
V: Electric voltage of the equipment [V];
I: Electric current measured during its operation [A].

Finally, calculation of the overall and hydraulic efficiency are performed by Eq. (7) and Eq. (8), where Y_{ideal} represents a situation where all mass entering the equipment is being effectively delivered in the outlet, this consideration will be discussed later.

$$\eta_t = \frac{P_{fluid}}{P_{ele}} \times 100 \tag{7}$$

$$\eta_h = \frac{Y_{fluid}}{Y_{ideal}} \times 100 \tag{8}$$

Since the equipment is focused on reducing the air temperature, another two coefficients need to be analyzed, the effectiveness (Eq. 9) and *EER* – Energy Efficiency Ratio, Eq. (10) (Effatnejad e Salehian, 2009):

$$\varepsilon = \frac{TBS_i - TBS_o}{TBS_i - TBU_i} \times 100 \tag{9}$$

TBS_i: Dry bulb temperature at the inlet [ºC]
TBS_o: Dry bulb temperature at the outlet [ºC]
TBU_i: Wet bulb temperature at the inlet [ºC]

$$EER = \frac{\dot{Q}_{dry\ air}}{P_e} \tag{10}$$

Where $\dot{Q}_{dry\ air}$ is defined as:

$$\dot{Q}_{dry\ air} = \dot{m}_{dry\ air} C_p (T_{in} - T_{out}) \tag{11}$$

The C_p was taken as the value obtained for 300K (since the C_p vary very little given our temperature range). Also, $\dot{m}_{dry\ air}$ was calculated subtracting the water content in the outlet air (using absolute humidity), from the calculated total mass flow, as:

$$\dot{m}_{dry\ air} = \dot{V}\left(1 - \frac{1}{(VE)_o}(UA)_o\right) \tag{12}$$

VE_o: Specific Volume at the outlet [m³/kg];
UA_o: Absolute Humidity at the outlet [kg_{vapor}/kg_{air}]

In order to classify the equipment, the specific speed; non-dimensional number (Henn, 2009) was also calculated, following Eq. (13):

$$n_{qA} = n\frac{\dot{V}^{\frac{1}{2}}}{Y^{\frac{3}{4}}} \tag{13}$$

n: Angular speed [rps].

For the inlet position, the velocity triangles considered that the inlet angle (α) is equal to 90° since there are no guideline blades before the rotor's inlet. To acquire all necessary data, the following iterative process was carried out:

1. Enter the measured U_i
2. Guess C_i
3. Calculate $W_i = (U_i + C_i)^{0.5}$
4. Calculate the estimated $\beta' = cos^{-1}(U_i / W_i)$
5. If the estimated $\beta' \neq \beta$ *(measured = 33°)*, guess another C_i

For the outlet position, the same idea applies. Since the measured velocity in the outlet was used to calculate the volumetric flow, it is considered the absolute meridional velocity ($C_{m,o}$), and using the rotor's tangential velocity (U_o) and the angle of the blades on the outlet (β), we're able to calculate the missing data, following the script:

1. Enter the measured U_o *and* $C_{m,o}$
2. Guess C_o
3. Calculate $C_{u,o} = (C_o^2 - C_m^2)^{0.5}$
4. Calculate $W_{u,o} = U_o + C_{u,o}$
5. Calculate the estimated $\beta' = tan^{-1}(W_{u,o} / C_{m,o})$
6. If the estimated $\beta' \neq \beta$ *(measured = 33°)*, guess another C_o

This proposed methodology and its convergence criteria, provides the real outlet velocity triangles for the inlet and outlet. Another possibility would be to assume that the flow machine is an ideal fan; in that case, the volumetric flow would be constant, since mass is conserved, and there are no substantial density changes during the cooling process. Eq. (14) represents the idea behind it. That way, the measured $C_{m,o}$ is not used in the calculation, but the calculated $C_{m,o}$'. Since airflow is constant through the machine, its volumetric efficiency is 100%, without any leakage in its casing.

$$C_{m,o}{}' = \frac{A_i C_{m,i}}{A_o} \tag{14}$$

3. PROTOTYPE MODEL

The model was extrapolated from 300 to 1400 RPM (300 RPM step) on the following properties: volumetric flow, consumed electric power, and specific energy. The model predictions could be compared with the experimental data obtained from 850 and 1020 RPM. This extrapolation was performed applying the similarity analysis, as proposed by Henn (2006). To execute the calculations, a point must be chosen, so the other points (rotor angular speeds) will be extrapolated based on this first given data. The select point was the second angular speed (960 RPM). The relations between the model and the prototypes (indicated by ‘), are shown in Eq. 15 to 17.

$$\dot{V}' = \dot{V}\left(\frac{n'}{n}\right) \tag{15}$$

$$Y' = Y\left(\frac{n'}{n}\right)^2 \tag{16}$$

$$P_e' = P_e\left(\frac{n'}{n}\right)^3 \tag{17}$$

4. RESULTS AND DISCUSSION

Table 4 summarizes the measured rotor angular speeds, in RPM and outlet airflow velocity.

Table 4. Rotor angular speeds and airflow velocity measurements

Position	1	2	3
Rotor: Angular speed (RPM)	844.5	964.6	1019.0
Air: Mean outlet velocity ($\overline{C_{m,o}}$) ± Uncertainty (m/s)	4.3 ± 0.33	5.1 ± 0.38	6.0 ± 0.35

After this step, the script was applied to proceed with the ideal velocity triangle. Figure 3 shows the results of this process. By the geometry of the outlet triangles, the director system in the outlet of the CFF changes the direction of the absolute velocity, turning it to go almost in the counter-clockwise direction. One could disregard the fixed outlet beta

angle to achieve more helpful and physically coherent triangles but with a random beta angle. Since we could not take measurements at the outlet tip of the blades, the angle achieved by disregarding the measured beta angle would be the one of the outlet flow outside the equipment, where the data is collected.

It's impossible to calculate this outlet angle since we only know $C_{m,o}$ and U_o. The equations system cannot be solved, and even guessing a C_o, there is no parameter of comparison to stop when the calculations have reached the expected result to W components, as the beta angle served in the proposed methodology.

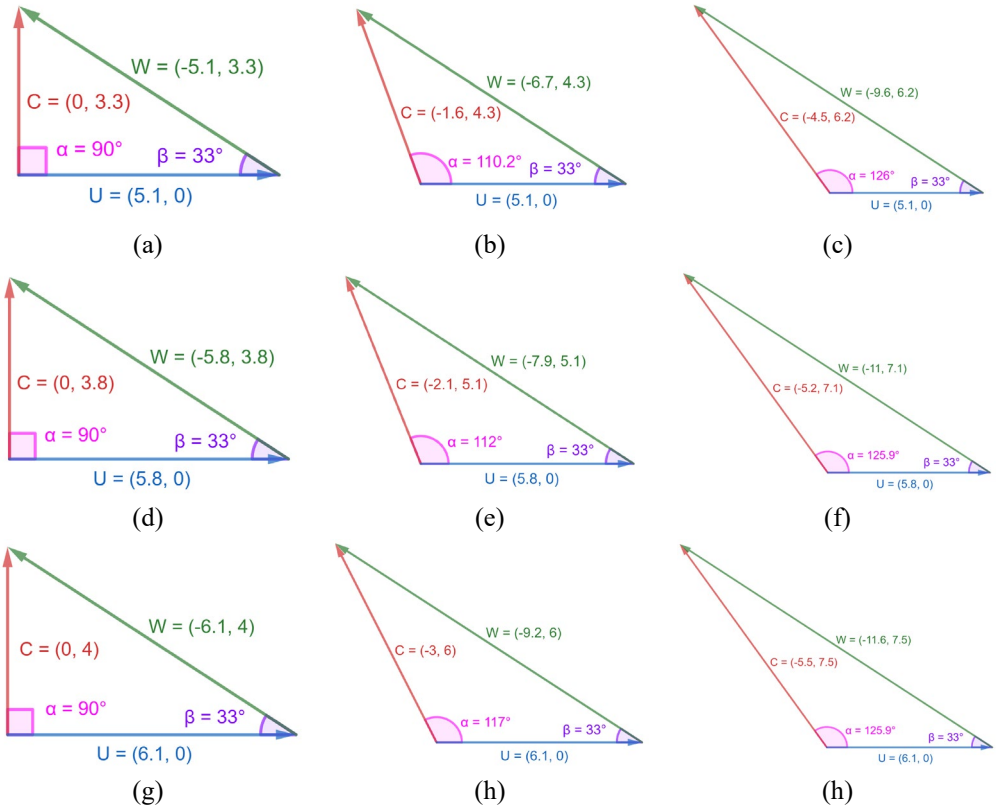

Figure 3. Velocity triangles, inlet, outlet – REAL, and outlet – IDEAL. In order: 850 RPM (a, b and c); 960 RPM (d, e and f), and 1020 RPM (g, h and i)

It is noticeable that there are several hydraulic losses in the machine since the final ideal absolute fluid velocity is much higher than when considering the real outlet measured velocity.

The results of outlet psychometric data are in Table 5. We can observe that the outlet temperature has decreased as the flow passed through the equipment. Along with the increase in the absolute and relative humidity.

Table 5. Measured and calculated (*) data.

RPM	844.5	964.6	1019
TBS,i (°C)	29.7	29.9	30.0
UR,i (%)	65.2	64.2	64.1
TBU,i (°C)*	24.5	24.5	24.5
UA,i (kg vapor/kg air)*	0.019	0.019	0.019
VE,i (m³/kg air)*	0.932	0.932	0.933
TBS,o (°C)	27.7	27.8	27.9
UA,o (kg vapor/kg air)	0.0211	0.0211	0.0213
UR,o (%)*	83.68	83.19	83.09
TBU,o (°C)*	25.46	25.49	25.57
UA,o (kg vapor/kg air)	0.0211	0.0211	0.0213
VE,o (m³/kg ar)*	0.929	0.930	0.930

The performance data is in Table 6. An interesting result is the overall efficiency, with surprisingly low values. It is the ratio between the energy the fluid receives divided by the amount the machine requires. It is logical to determine the final flow energy is not as high as it could be. With the ideal approach, the overall efficiency didn't increase much,

reaching a maximum of 17%. The maximum overall efficiency apparently does not occur in the operational range, as it is almost constant in the tested interval.

Another significant remark is that the total kinetic energy provided by the CFF is not relevant compared with the thermal energy exchanged with the airflow. For the first rotor angular speed, it is equivalent to only 0.42% (0.88% for the highest velocity) of the thermal energy rate. The total energy rate increases with the mass flow rate, but the effectiveness remains constant since the temperature change (inlet – outlet) is practically the same for all angular velocities. Using the classification proposed by Torkaman e Ghassembaglou (2015), for an $EER < 26$, the analyzed machine is in the 7G classification, the worst rating. It only corroborates the fact that the overall performance of the CFF is not close to the ideal.

Table 6. Performance data of the equipment

RPM	844.5	964.6	1019
ε	39%	39%	39%
$\dot{V}_{humid\ air}$ (m³/h)	318	374	436
$\dot{m}_{water}$ (kg/h)	0.708	0.837	1.083
$\dot{m}_{humid\ air}$ (kg/h)	342	402	469
$\dot{m}_{dry\ air}$ (kg/h)	335	394	459
$\dot{V}_{dry\ air}$ (m³/h)	311	366	426
$\dot{Q}_{dry\ air}$ (kW)	0.1897	0.2343	0.2731
P (kW)	0.0127	0.0254	0.0381
EER	14.94	9.22	7.17
Y_{fluid} (J/kg)	8.1	11.9	18.6
P_{fluid} (W)	0.8	1.3	2.4
η_t	6%	5%	6%
η_h	35%	40%	55%

The volumetric airflow informed by the manufacturer is 350 m³/h; so, the values calculated by the three rotor angular speeds seem acceptable in comparison to that. The power consumption of the machine is 75 W, following the datasheet, and it was not achieved during the tests, the maximum measured electrical power was 38.1 W, for the maximum air flow velocity.

Figure 4 shows the extrapolation for several rotor angular speeds (the apostrophe represents the model). It is possible to infer that for velocities below 1000 RPM, the model is accurate, but in comparison with the results obtained for 1020 RPM, it's clearly not following the same pattern. A plausible interpretation, is that the model cannot compute the interference of the losses correctly, not being able to predict the behavior of the CFF at higher speeds, where it has a higher hydraulic efficiency; that could also be related to higher or lower hydraulic losses.

If we set the base value for the model as the data obtained to 1020 RPM, we would see a different tendency, as it has a higher hydraulic efficiency and would also predict the lower rotor angular speeds to have higher property values.

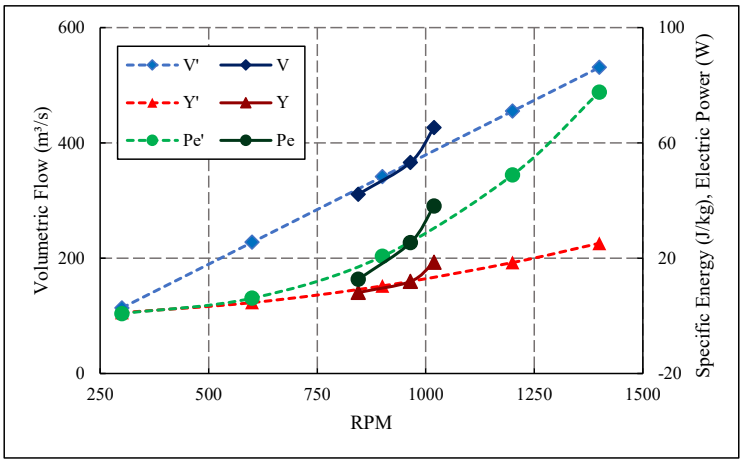

Figure 4. Prototype extrapolation analysis in comparison with real data

Following, nqA values are in Figure 5. The results obtained for the specific speed (nqA) can be compared to those shown by Henn (2006), labeling the fluid machine as similar to centrifugal fans with an outlet blade angle of 90º (nqA = 50) but different from these machines, the crossflow fan static pressure rise is said to be negligible ($\Delta p_{static} \approx 0$). For

centrifugal fans and turbocompressors, the *nqA* is between 20 and 330. On the other hand, for axial fans or turbocompressors, it would be between 330 and 1800. Therefore, the crossflow fan category would be closer to that attributed to the centrifugal fluid machines. It makes sense, given the geometry of the equipment.

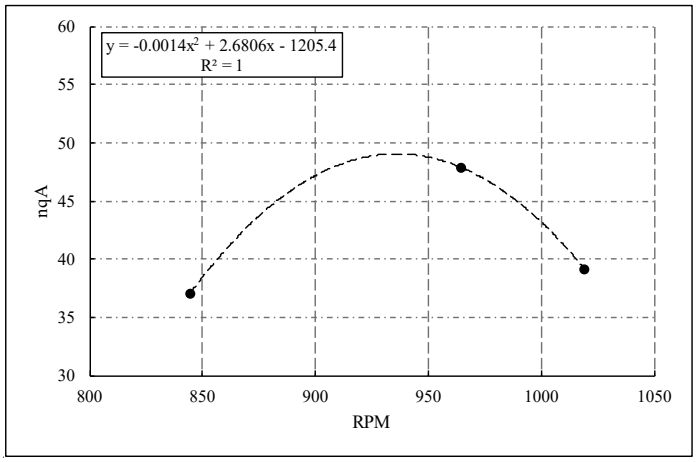

Figure 5. Specific speed (nq-A)

From the displayed analysis, a new concern arises. Contrasting to an air-conditioner or a common fan, the evaporative coolers cannot be evaluated only based on the air's temperature decrease or the energy given to the fluid. A more concise analysis should consider both of them to fully evaluate the intrinsic characteristics of the EC. The authors propose a new adimensional coefficient called COP_{EC} (*COP* Evaporative Cooler). It can be defined by Eq. 18.

$$COP_{EC} = \frac{\dot{Q}_{dry\ air} + P_{fluid}}{P_{ele}} \tag{18}$$

Even though, as presented, the energy given to the fluid is irrelevant compared to the thermal energy, it is a particular case for this equipment and cannot be generalized since it can represent a notable portion. Figure 6 shows the results. For standardization, extensive research should be developed, adopting the guidelines established in this work so one could compare several machines based on their COP_{EC}.

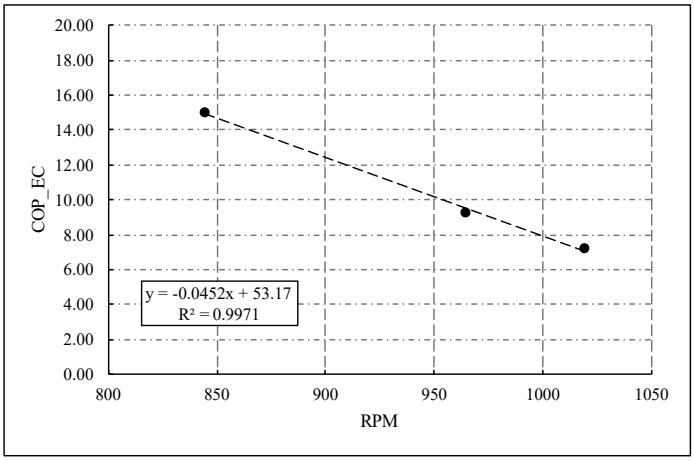

Figure 6. COP_{EC} achieved for each angular speed

5. CONCLUSION

In the main findings in this work, it's not possible to identify maximum performance in the operational angular speeds, since η_{max} remains almost constant. Also, the CFF kinetic energy is negligible in comparison to thermal energy in small evaporative coolers (EC).

Using similarity analysis, we could achieve reliable results for rotations lower than the used for the model, but the differences when extrapolating for higher rotations was considerable high, when compared to measured data. In

experimental results for airflow values at the maximum rotor angular speed are consistent with nominal values provided by the manufacturer. The machine has poor energy efficiency and many sources for hydraulic losses, which should be improved to achieve higher levels of energy efficiency. Since it lacks a standard method of classification, we advise to take a closer look at this kind of equipment.

The CFF *nqA* characteristics are similar to those associated with centrifugal fans and compressors, due to the low *nqA* values obtained and the similarity of the machine rotor and casing. A new adimensional aroused, COP_{EC}, allows the evaluation of different ECs, based on both the energy the air receives from the blades and the air temperature reduction, the authors encourage the use of this new coefficient to evaluate several different ECs, establishing the equipment classes based on their efficiency (as already exists for other kinds of household equipment with the PROCEL seal.

6. ACKNOWLEDGEMENTS

We thank UFGD and CNPq for the scholarships for undergraduate engineering students (IC & ITI). To CAPES for support in PEM / UEM (Graduate Program in Mechanical Engineering / Maringá State University), and UNICAMP for the resources provided to first author to present this work.

7. REFERENCES

Albertazzi, A., Souza, A. R., 2018. *Fundamentals of scientific and industrial metrology (in Portuguese)*. Publisher Manole, São Paulo. ISBN: 978-85-204-3375-1.

Balbinot, A., & Brusamarello, V. J., 2010. *Instrumentation and measurement fundamentals (in Portuguese)*. Rio de Janeiro, RJ: LTC, vol. 1, 2nd ed. 385p.

Dragomirescu, A., Ciocãnea, A., 2015. “Enhancing the efficiency of indoor local ventilation using crossflow fans: Case study for a smoking cabin”. In Journal of Engineering Studies and Research, Vol. 21, No. 3, pp. 28–34. DOI: Not Available.

Effatnejad, R., Salehian, A. B., 2009. "TANDARD OF ENERGY CONSUMPTION AND ENERGY LABELING IN EVAPORATIVE AIR COOLER IN IRAN". In International Journal on “Technical and Physical Problems of Engineering” (IJTPE), Vol. 1, Issue 1, Number 1, pp. 54-57.

Gebrehiwot, M.G., Baerdemaeker, J.D., Baelmans, M., 2010. “Numerical and experimental study of a crossflow fan for combine cleaning shoes”. In Biosystems Engineering, Vol. 106, No. 4, pp. 448–457. DOI: https://doi.org/10.1016/j.biosystemseng.2010.05.009.

Koo, H., 1999. "An experimental study of the noise and the performance of crossflow fans in room air-conditioning systems". In Noise Control Engineering Journal, Vol. 48, Number 2, pp. 41-47. DOI: https://doi.org/10.3397/1.2827973.

Henn, E.A L., 2006. *Fluid Machinery (in Portuguese).* Santa Maria, RS: Ed. UFSM, 2nd ed. 474p.

Neto, J. C. S., 2012. *Metrology and Dimensional Control (in Portuguese).* Elsevier Publisher Ltda, Rio de Janeiro. ISBN: 978-85-352-5579-9

Porter, A. M., Markland, E., 1970. "A Study of the Cross Flow Fan". In Journal of Mechanical Engineering Science, Vol. 12, Issue 6. DOI: https://doi.org/10.1243/JMES_JOUR_1970_012_071_02.

Sun, K., Ouyang, H., Tian, J., Wu, Y., Du, Z., 2015. “Experimental and numerical investigations on the eccentric vortex of the crossflow fan”. In International Journal of Refrigeration, Vol. 50, No. 2, pp. 146–155. DOI: https://doi.org/10.1016/j.ijrefrig.2014.10.005.

Tanaka, S., Murata, S., 1995. "Scale Effects in Cross Flow Fans: Effects of Fan Dimensions on Flow Details and the Universal Representation of Performances". In JSME International Journal Series B Fluids and Thermal Engineering, Vol. 38, Issue 3, pp. 388-397. DOI: https://doi.org/10.1299/jsmeb.38.388.

Torkaman, L., Ghassembaglou, N., 2015. “Evaporative aircoolers optimization for energy consumption reductionand energy efficiency ratio increment”. In Int. J. Mec. MechaEng., Vol. 9, Issue 4, pp. 622-627. DOI: 10.5281/zenodo.110054.

Ventisol, 2023, *CLM-01 datasheet (in Portuguese)*, https://www.agrotama.com.br/upload/album/arquivo_manual179_1.pdf. Accessed 01 April 2023.

Yamafuji, K., 1975. "Studies on the Flow of Crossflow Impellers: 1st Report, Experimental Study". In Bulletin of JSME, Vol. 18, Issue 123, pp. 1018-1025. DOI: https://doi.org/10.1299/jsme1958.18.1018.

8. RESPONSIBILITY NOTICE

The authors are the only responsible for the printed material included in this paper.